Throughput Optimization for NOMA Cognitive Radios with Multi-UAV Assisted Relay

Le-Mai-Duyen Nguyen[1,2], Van Nhan Vo[2,3(✉)], Tran Thi Thanh Lan[2,3], Nguyen Minh Nhat[2,3], Anand Nayyar[2,3], and Viet-Hung Dang[2,3]

[1] Faculty of Electrical-Electronic Engineering, Duy Tan University, Da Nang 550000, Vietnam
nguyenlmaiduyen@duytan.edu.vn
[2] Institute of Research and Development, Duy Tan University, Da Nang 550000, Vietnam
vonhanvan@dtu.edu.vn, {tranthithanhlan,nguyenminhnhat, anandnayyar,dangviethung}@duytan.edu.vn
[3] Faculty of Information Technology, Duy Tan University, Da Nang 550000, Vietnam

Abstract. In this paper, we investigate the throughput optimization for the non-orthogonal multiple access (NOMA) cognitive radio (CR) system with multi-unmanned aerial vehicle (UAV) assisted relays. We propose the communication protocol as follows: in the first phase, a secondary transmitter (ST) transmits the signals to the first UAV relay (UR) using non-orthogonal multiple access (NOMA); meanwhile, a ground base station (GBS) communicates with a primary receiver (PR) under the interference of the ST. In the second phase, the first UR applies the decode-and-forward (DF) technique to transfer the signals to the second UR. Simultaneously, the GBS communicates with PR under the interference of the first UR. Similarly, in the next phase, the UR forwards the signals, while the PR receives the information from the GBS without the interference. In the last two phases, the UR and the SRs receive the signals under the GBS's interference. Accordingly, the outage probability of the primary network and the throughput of the secondary network is analyzed. Moreover, we propose constraint genetic algorithm (CGA) aided obtaining UR's configurations to optimize the throughput of the secondary network under the constraints of the system performance of the primary network.

Keywords: Cognitive Radio (CR) · Non-Orthogonal Multiple Access (NOMA) · Unmanned Aerial Vehicle (UAV) · Continuous Genetic Algorithm (CGA) · UAV Relay (UR)

1 Introduction

The cognitive radio (CR) is widely regarded as a potential solution for addressing the issues of spectrum scarcity, which have been exacerbated by the enormous

N.-S. Vo et al. (Eds.): INISCOM 2022, LNICST 444, pp. 91–104, 2022.
https://doi.org/10.1007/978-3-031-08878-0_7

development of wireless data traffic of the fifth generation (5G) communication systems [9]. More specifically, CR allows public access to the underutilized spectral bands in order for unlicensed (cognitive) users to exploit the licensed spectrum from an opportunistic point of view, thus economically increasing overall spectral efficiency [10].

On the other hand, the above requirements for 5G systems, especially spectrum efficiency and huge connectivity, non-orthogonal multiple access (NOMA) can be a supplement solution for CR technique because it demonstrates the capacity to boost connection if there are restricted radio resources available [14]. In NOMA, the whole bandwidth may be used simultaneously by each user with different power levels [13].

For example, the authors in [4] investigated a relaying scheme in the cooperative NOMA CR with a primary transmitter (PT), a primary receiver (PR), a secondary transmitter (ST), a relay, and two secondary receivers (SRs). The closed-form expressions for outage probability (OP) are derived for evaluating the system performance of the two SRs over both Rayleigh fading and Nakagami-m fading. For extension, Z. Xiang *et al.* considered a NOMA CR network with a a PT, a ST, multiple PRs, and multiple SRs. The authors concluded that the NOMA and CR combination can reduce the mutual interference among signals and improve the system throughput for massive users [14].

However, the large-scale connections with obstacle issues in CR networks lead to the reduction of system throughput. Thus, unmanned aerial vehicle (UAV) assisted relay is an effective means of improving the system performance. Thanks to the ability of overcoming obstacles and the flexibility to shift postures, UAV increases the possibility of line-of-sight (LoS) [6,11]. For example, L. Sboui *et al.* investigated the achievable rates of a CR with a UAV assisted relay. The authors derived the expression of the power maximizing both primary and secondary rates to analyze the system performance. They concluded that the UAV assisted relay may be used in conjunction with CR technology to increase both rates by using the flexibility, independence, and other quality of service (QoS) of UAVs [11].

Meanwhile, D. Chi-Nguyen *et al.* focused on a CR network where UAV is used as a relay to bridge the communication from a ST to a SR. Then, an optimization algorithm is proposed to achieve an optimal secrecy rate for the UAV CR network. The numerical results showed that the algorithm can achieve a fast coverage rate and optimize the UAV path [3]. It is noted that the interference from primary network to secondary network was not considered in this work. Therefore, B. Ji *et al.* investigated the interference issue of a cooperative transmission mechanism for a CR network, in which the primary network and the secondary network shared a dedicated radio frequency (RF) source with decode-and-forward (DF) UAV selection. The numerical results of the simulation verified the mechanism's efficiency and the calculation correctness [5].

However, based on the above survey, no existing work using multi-hop UAV relay (UR) in NOMA CR networks has studied the system performance optimization of the secondary network under the constraint OP of the primary network. This work will overcome those mentioned drawbacks with following primary contributions:

– We investigate a NOMA CR system, in which the ground base station (GBS) sends the signals to the PR using orthogonal multiple access (OMA) and the ST, with the help of multiple URs, transmits the information to the IoT destinations (IDs) using NOMA.
– We propose the communication protocol for the considered system and analyse the system performance at the primary and secondary networks.
– We propose to apply a CGA for resource allocation optimization of the URs such that the PR can decode the signals from the GBS.

2 System Model and Communication Protocol

2.1 System Model and Channel Assumptions

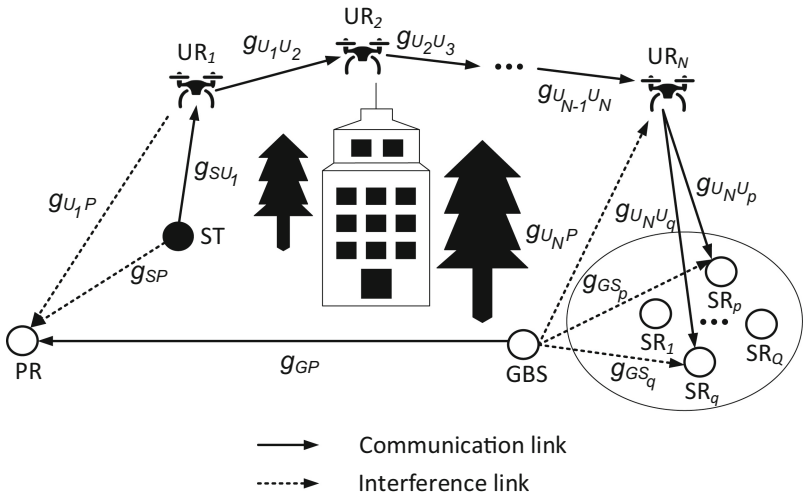

Fig. 1. A NOMA CR Internet of Things (IoT) architecture.

This paper aims to investigate the disturbed communication in a disaster situation when the GBS is no longer available for transferring the information to the IDs in the existing CR. Thus, let us consider a NOMA CR as shown in Fig. 1 in which primary users (PUs) (GBS and PR) licensed the spectrum by using OMA principle. Meanwhile, secondary users (SUs) ((ST, URs, and IDs, i.e., D_p and D_q) try to utilize the licensed spectrum by using NOMA technique for their communication provided that their transmit power does not interrupt the communication of the PUs. The GBS, PR, ST, IDs, URs are equipped with single antennas. Here, the channel gains and distances of GBS-PR, ST-PR, ST-UR_1, UR_1-PR, UR_n-$\text{UR}_n + 1$, UR_N-D_p, UR_N-D_q, GBS-UR_N, GBS-D_p, and GBS-D_p links are denoted by g_{GP}, g_{SP}, g_{SU_1}, $g_{U_nU_{n+1}}$, $g_{U_ND_p}$, $g_{U_ND_p}$, g_{GU_N}, g_{GD_p}, and

g_{GD_q}; and d_{GP}, d_{SP}, d_{SU_1}, $d_{U_nU_{n+1}}$, $d_{U_ND_p}$, $d_{U_ND_p}$, d_{GU_N}, d_{GD_p}, and d_{GD_q}, respectively, where N is the number of the URs and $n \in \{1, \ldots, N\}$.

Here, all channel gains are identically independent distributed (i.i.d) and remain constants for the duration of one packet. In particular, for the ground-to-ground communication, the channel gains are modeled as the gains of Rayleigh fading channels, i.e., random variables (RVs) distributed following an exponential distribution. Thus, the probability density function (PDF) and cumulative distribution function (CDF) of the channel gains are formulated as follows [6]:

$$f_{g_a}(x) = \frac{1}{\Omega_a} \exp\left(-\frac{x}{\Omega_a}\right), \tag{1}$$

$$F_{g_a}(x) = 1 - \exp\left(-\frac{x}{\Omega_a}\right), \tag{2}$$

where $a \in \{SP, GP, GD_p, GD_q\}$ is an RV with a mean value of $\Omega_a = \mathbf{E}[a]$.

For the air-to-ground and ground-to-air communication, the path loss models are expressed as absolute values

$$\overline{L}_b = \beta_b d_b^{\eta_b}, \tag{3}$$

where $b \in \{SU_1, U_ND_p, U_ND_q\}$. According to [8], a ground-to-air channel is more likely to be dominated by either LoS conditions or non-line-of-sight (NLoS) conditions depending on the environment (e.g., sub-urban, urban, or dense-urban). Here, we assume that $\eta_b = 2$; thus, the quantity β_b is formulated as $\beta_b = 10^B$ [2], in which B is defined as

$$\begin{aligned} B =& \frac{10\log_{10}\left(4\pi f/c\right)^2 + \omega_{NLoS}}{10} \\ &+ \frac{\omega_{LoS} - \omega_{NLoS}}{10 + 10\varphi\exp\left[-\psi\left(\frac{180}{\pi}\theta - \varphi\right)\right]}, \end{aligned} \tag{4}$$

where θ is the UR elevation angle with respect to either the GBS, ST, or IDs; φ and ψ are constants that depend on the environment [12]; and ω_{LoS} and ω_{NLoS} are environment and frequency dependent parameters that represent the excess path losses of the LoS link and NLoS link, respectively [12]. For the air-to-air communication, the path loss can be expressed as [2]

$$\overline{L}_{U_nU_{n+1}} = \beta_{U_nU_{n+1}} d_{U_nU_{n+1}}^{\eta_{U_nU_{n+1}}}, \tag{5}$$

where $\beta_{U_nU_{n+1}} = \left(\frac{4\pi f}{c}\right)^2$.

Furthermore, the ground-to-air, air-to-ground, and air-to-air channel gains follow Nakagami-m distributed fading environment with fading severity parameter m [7], i.e., RVs following a Gamma distribution. Thus, the PDF and CDF of channel gain g_α are formulated as follows [6]:

$$f_{g_\alpha}(x) = \left(\frac{m_\alpha}{\Omega_\alpha}\right)^{m_\alpha} \frac{x^{m_\alpha - 1}}{\Gamma(m_\alpha)} \exp\left(-\frac{m_\alpha x}{\Omega_\alpha}\right), \tag{6}$$

$$F_{g_\alpha}(x) = 1 - \sum_{j=0}^{m_\alpha - 1} \left(\frac{m_\alpha x}{\Omega_\alpha}\right)^j \frac{1}{j!} \exp\left(-\frac{m_\alpha x}{\Omega_\alpha}\right). \tag{7}$$

where $\alpha \in \{b, U_n U_{n+1}\}$, g_α is a RV with a mean value $\Omega_\alpha = \mathbf{E}\left[|g_\alpha|^2\right]$ and $\Gamma(\cdot)$ is the Gamma function. In addition, due to the complex environment, the imperfect channel state information (CSI) is considered for all channels, i.e., $g_a = \tilde{g}_a + e_a$ and $g_\alpha = \tilde{g}_\alpha + e_\alpha$, where $\tilde{g}_a$ and $\tilde{g}_\alpha$ are the channel coefficients estimated by using the minimum mean square errors (MMSEs) for g_a and g_α, respectively; and $e_a, e_\alpha \sim \mathcal{CN}(0, \Omega_e)$, with Ω_e being the correctness of the channel estimation and $\mathcal{CN}(0, \Omega_e)$ being a scalar complex Gaussian distribution with zero mean and variance Ω_e [1].

2.2 Communication Protocol

The basic idea of a NOMA CR is that the GBS with the transmitted power P_P sends the signal to the PR on an orthogonal frequency band in the primary network. For the secondary network, the ST may sense the frequency band from the GBS to transmit the signals to D_p and D_q with the help of the URs by applying NOMA principle. Specifically, there are $(N+1)$ phases for signal transmission from the GBS to the IDs as follows:

– In the first phase, the ST transmits the superimposed signal x_S to D_p and D_q, where $x_S = \sqrt{\mu_p} x_p + \sqrt{\mu_q} x_q$, $\mu_p + \mu_q = 1$, and $\mu_p < \mu_q$. Therefore, the received signal at the first UR can be written as

$$y_{U_1} = \sqrt{\frac{P_S}{\bar{L}^\theta_{SU_1}}} \left(\sqrt{\mu_p} x_p + \sqrt{\mu_q} x_q\right) g_{SU_1} + n_{U_1}, \tag{8}$$

where $n_{U_1} \sim \mathcal{CN}(0, N_0)$. The received signal-to-interference-plus-noise ratios (SINRs) at the first UR for decoding x_p and x_q are formulated as

$$\gamma^{(p)}_{U_1} = \frac{\mu_p P_S \tilde{g}_{SU_1}}{\bar{L}_{SU_1}(P_S \Omega_e + N_0)}, \tag{9}$$

$$\gamma^{(q)}_{U_1} = \frac{\mu_q P_S \tilde{g}_{SU_1}}{\bar{L}_{SU_1}\left(\frac{\mu_p P_S \tilde{g}_{SU_1}}{\bar{L}_{SU_1}} + P_S \Omega_e + N_0\right)}. \tag{10}$$

Meanwhile, the GBS broadcasts the signal x_P to the PR by using OMA principle. It is noted that the ST interferes the PR on the orthogonal frequency

band due to the broadcast nature. Thus, the received signal at the PR in the first phase can be written as

$$y_P^{(1)} = \sqrt{\frac{P_P}{d_{GP}^{\theta}}} g_{GP} x_P + \sqrt{\frac{P_S}{d_{SP}^{\theta}}} g_{SP} x_S + n_P^{(1)}, \tag{11}$$

where $n_P^{(1)} \sim \mathcal{CN}(0, N_0)$. Therefore, the received SINR at the PR is formulated as

$$\gamma_P^{(1)} = \frac{P_P \tilde{g}_{GP}}{d_{GP}^{\theta} \left[\frac{P_S \tilde{g}_{SP}}{d_{SP}^{\theta}} + (P_S + P_P) \Omega_e + N_0 \right]}. \tag{12}$$

– In the second phase, the first UR uses the DF to decode and forward the signal from ST to the second UR. Thus, the received signal at the second UR can be written as

$$y_{U_2} = \sqrt{\frac{P_{U_1}}{\bar{L}_{U_1U_2}^{\theta}}} \left(\sqrt{\mu_p^{(1)}} x_p + \sqrt{\mu_q^{(1)}} x_q \right) g_{U_1U_2} + n_{U_2}, \tag{13}$$

where $n_{R_2} \sim \mathcal{CN}(0, N_0)$. Therefore, the received SINRs at the second UR for decoding x_p and x_q are formulated as

$$\gamma_{U_2}^{(p)} = \frac{\mu_p^{(1)} P_{U_1} \tilde{g}_{U_1U_2}}{\bar{L}_{U_1U_2} (P_{U_1} \Omega_e + N_0)}, \tag{14}$$

$$\gamma_{U_2}^{(q)} = \frac{\mu_q^{(1)} P_{U_1} \tilde{g}_{U_1U_2}}{\bar{L}_{U_1U_2} \left(\frac{\mu_p^{(1)} P_{U_1} \tilde{g}_{U_1U_2}}{\bar{L}_{U_1U_2}} + P_{U_1} \Omega_e + N_0 \right)}. \tag{15}$$

Furthermore, due to the short distance from the first UR to the PR, the interference of the UR affects the received signal at the PR as follows:

$$y_P^{(2)} = \sqrt{\frac{P_P}{d_{GP}^{\theta}}} g_{GP} x_P + \sqrt{\frac{P_{U_1}}{d_{U_1P}^{\theta}}} g_{U_1P} x_S + n_P^{(2)}, \tag{16}$$

where $n_P^{(2)} \sim \mathcal{CN}(0, N_0)$. Therefore, the received SINR at the PR in the second phase is formulated as

$$\gamma_P^{(2)} = \frac{P_P \tilde{g}_{GP}}{d_{GP}^{\theta} \left[\frac{P_{U_1} \tilde{g}_{U_1P}}{\bar{L}_{U_1P}^{\theta}} + (P_{U_1} + P_P) \Omega_e + N_0 \right]}. \tag{17}$$

– Similarly, in the n-th phase ($2 < n < N$), the $(n-1)$-th UR decodes and forwards the signal from the $(n-2)$-th UR to the n-th UR. Thus, the received signal at the n-th UR can be written as

$$y_{U_n} = \sqrt{\frac{P_{U_{n-1}}}{\bar{L}_{U_{n-1}U_n}^{\theta}}} \left(\sqrt{\mu_p^{(n-1)}} x_p + \sqrt{\mu_q^{(n-1)}} x_q \right) \times g_{U_{n-1}U_n} + n_{U_n}, \tag{18}$$

where $n_{U_n} \sim \mathcal{CN}(0, N_0)$. Then, the received SINRs at the n-th UR for decoding x_p and x_q are formulated as

$$\gamma_{U_n}^{(p)} = \frac{\mu_p^{(n)} P_{U_{n-1}} \tilde{g}_{U_{n-1}U_n}}{\bar{L}_{U_{n-1}U_n} \left(P_{U_{n-1}} \Omega_e + N_0\right)}, \tag{19}$$

$$\gamma_{U_n}^{(q)} = \frac{\mu_q^{(n)} P_{U_{n-1}} \tilde{g}_{U_{n-1}U_n}}{\bar{L}_{U_{n-1}U_n} \left(\frac{\mu_p^{(n)} P_{U_{n-1}} \tilde{g}_{U_{n-1}U_n}}{\bar{L}_{U_{n-1}U_n}} + P_{U_{n-1}} \Omega_e + N_0\right)}. \tag{20}$$

For the primary network, the received signal at the PR in the n-th phase is written as

$$y_P^{(n)} = \sqrt{\frac{P_P}{d_{GP}^{\theta}}} g_{GP} x_P + n_P^{(n)}, \tag{21}$$

where $n_P^{(n)} \sim \mathcal{CN}(0, N_0)$. The received SINR at the PR in the n-th phase is

$$\gamma_P^{(n)} = \frac{P_P \tilde{g}_{GP}}{d_{GP}^{\theta} \left(P_P \Omega_e + N_0\right)}. \tag{22}$$

– In the N-th and $(N+1)$ slots, the N-th UR and the IDs are affected by the interference of the GBS because of the broadcast nature. Thus, the received signals at the N-th UR, D_p, and D_q, respectively, become

$$y_{U_N} = \sqrt{\frac{P_{U_{N-1}}}{\bar{L}_{U_{N-1}U_N}}} g_{U_{N-1}U_N} x_S + \sqrt{\frac{P_P}{d_{GU_N}^{\theta}}} g_{GU_N} x_P + n_{U_N}, \tag{23}$$

$$y_{D_p} = \sqrt{\frac{P_{U_N}}{\bar{L}_{U_N}}} g_{U_N} x_S + \sqrt{\frac{P_P}{d_{GD_p}^{\theta}}} g_{GD_p} x_P + n_{D_p}, \tag{24}$$

$$y_{D_q} = \sqrt{\frac{P_{U_N}}{\bar{L}_{U_N D_q}}} g_{U_N D_q} x_S + \sqrt{\frac{P_P}{d_{GD_q}^{\theta}}} g_{GD_q} x_P + n_{D_q}, \tag{25}$$

where $n_{U_N}, n_{D_p}, n_{D_q} \sim \mathcal{CN}(0, N_0)$. Accordingly, the SINRs at U_N, D_p, and D_q for decoding the p-th and q-th signals are

$$\gamma_{U_N}^{(p)} = \frac{\mu_p^{(N-1)} P_{U_{N-1}} \tilde{g}_{U_{N-1}U_N}}{\bar{L}_{U_{N-1}U_N} \left[\begin{array}{l} \frac{P_P \tilde{g}_{GU_N}}{\bar{L}_{GU_N}} + N_0 \\ + \left(P_P + P_{U_{N-1}}\right) \Omega_e \end{array}\right]}, \tag{26}$$

$$\gamma_{U_N}^{(q)} = \frac{\mu_q^{(N-1)} P_{U_{N-1}} \tilde{g}_{U_{N-1}U_N}}{\bar{L}_{U_{N-1}U_N} \left[\begin{array}{l} \frac{\mu_p^{(N-1)} P_{U_{N-1}} \tilde{g}_{U_{N-1}U_N}}{\bar{L}_{U_{N-1}U_N}} + N_0 \\ + \frac{P_P \tilde{g}_{GU_N}}{\bar{L}_{GU_N}} + \left(P_P + P_{U_{N-1}}\right) \Omega_e \end{array} \right]}, \tag{27}$$

$$\gamma_{D_p}^{(p)} = \frac{\mu_p^{(N)} P_{U_N} \tilde{g}_{U_N D_p}}{\bar{L}_{U_N D_p} \left[\frac{P_P \tilde{g}_{GD_p}}{d_{GD_p}^{\theta}} + \left(P_P + P_{U_N}\right) \Omega_e + N_0 \right]}, \tag{28}$$

$$\gamma_{D_q}^{(q)} = \frac{\mu_q^{(N)} P_{U_N} \tilde{g}_{U_N D_q}}{\bar{L}_{U_N D_q} \left[\begin{array}{l} \frac{\mu_p^{(N)} P_{U_N} \tilde{g}_{U_N D_q}}{\bar{L}_{U_N D_q}} + \frac{P_P \tilde{g}_{PD_q}}{d_{PD_q}^{\theta}} \\ + \left(P_P + P_{U_N}\right) \Omega_e + N_0 \end{array} \right]}. \tag{29}$$

Similar to the n-th phase, the received signals at the PR in the N-th and $(N+1)$-th phase are not affected by the interference from the GBS. In other words, the received SINRs at the PR in the $(N+1)$-th phase are

$$\gamma_P^{(N)} = \gamma_P^{(N+1)} = \gamma_P^{(n)}. \tag{30}$$

According to the DF definition, the end-to-end SINRs for decoding the signals at the p-th and q-th ID are as follows:

$$\gamma_{E2E}^{(p)} = \min\left\{\gamma_U^{(p)}, \gamma_{D_p}^{(p)}\right\}, \tag{31}$$

$$\gamma_{E2E}^{(q)} = \min\left\{\gamma_U^{(q)}, \gamma_{D_q}^{(q)}\right\}, \tag{32}$$

where $\gamma_U^{(p)} = \min\limits_{n\in\{1,\ldots,N\}} \gamma_{U_n}^{(p)}$ and $\gamma_U^{(q)} = \min\limits_{n\in\{1,\ldots,N\}} \gamma_{U_n}^{(q)}$.

3 System Performance Analysis and Problem Formulation

In this section, the system performance of the NOMA CR is analyzed. Then, the problem formulation is defined in which the ST and the URs need to control their power allocations for satisfying that the communication from the GBS to the PR does not degrade and the throughput of the secondary network is maximized.

In order to guarantee the above conditions, the OP of the PR in all phases should be smaller than a predefined threshold, ε_P, i.e.,

$$\mathcal{O}_P = \Pr\left\{C_P < \gamma_P\right\} \leq \varepsilon_P, \tag{33}$$

where γ_P is the outage threshold at the PR and C_P is the channel capacity of the GBS-PR link with the bandwidth system (W) as follows:

$$\begin{aligned} C_P &= \min_{n\in\{1,\ldots,N+1\}} C_P^{(n)} \\ &= \min_{n\in\{1,\ldots,N+1\}} \frac{W}{N+1} \log\left(1+\gamma_P^{(n)}\right). \end{aligned} \tag{34}$$

Furthermore, the OP of the secondary network is formulated as follows:

$$\mathcal{O}_S = \Pr\left\{C_S^{(p)} < \gamma_S \text{ or } C_S^{(q)} < \gamma_S\right\}, \tag{35}$$

where γ_S is the outage threshold at the IDs and $C_S^{(p)}$ and $C_S^{(q)}$ is the channel capacities of the ST-D_p and ST-D_q links as follows:

$$C_S^{(p)} = \frac{W}{N+1}\log\left(1+\gamma_{E2E}^{(p)}\right), \tag{36}$$

$$C_S^{(q)} = \frac{W}{N+1}\log\left(1+\gamma_{E2E}^{(q)}\right). \tag{37}$$

Then, the throughput of the secondary network is defined as follows:

$$\mathcal{T}_S = (1-\mathcal{O}_S)\,\gamma_S. \tag{38}$$

The objective is to maximize the throughput of the secondary network subject to the requirements of the OP of the primary network. In particular, we optimize the power allocation factors at the URs, i.e., μ_p, $\mu_p^{(n)}$, and the altitudes of the URs. Then, the optimization problem can be formulated as follows:

$$\max_{\mu_p,\mu_p^{(n)},h_n} \{\mathcal{T}_S\}, \tag{39}$$

$$\text{s.t. } P_S \le P_{\max}, \tag{40}$$

$$\mathcal{O}_P^{(n)} \le \varepsilon_P, \tag{41}$$

$$\mu_p + \mu_q = 1, \tag{42}$$

$$\mu_p^{(n)} + \mu_q^{(n)} = 1, \tag{43}$$

$$n \in \{1,\ldots,N+1\}, \tag{44}$$

where $P_{\max}$ is the maximum transmit power of the ST.

4 CGA Aided Optimum Power Allocation and URs' Altitudes

The given problem in (39)–(44) is a nonlinear optimization problem which can be solved by optimization methods including calculus-based, exhaustive search, and sub-optimal search. Calculus-based is suitable for convex objective functions but not applicable for non-convex and multi-optima ones. Meanwhile, exhaustive search takes high computational cost and long run time with high dimension search space. Therefore, in this work, we apply Continuous Genetic Algorithm (CGA), a heuristic sub-optimal optimization method, which can deal with non-convex function and high dimension input. The searched parameters are power allocations and the altitudes of UAVs which try to maximize the system throughput.

Algorithm 1. Continuous Genetic Algorithm

Initialize
$t = 0$, λ, r_c, r_m, and T
\\T is the maximum number of generation iterations
Generate initial population $\mathbf{d}_k^{(t)}, k = 1, \ldots, \lambda$
for ($t = 1$ to T) **do**
  for ($k = 1$ to λ) **do**
    Evaluate fitness of chromosome k: $\mathbf{f_k^{(t)}} = \mathcal{T}_S$ as in (38)
  end for
  Reproduce chromosomes based on their fitnesses
  Apply crossover by pairing the parents with r_c
  Apply mutation to offspring with r_m
  \\New population is formed
end for
Output the best chromosomes

CGA algorithm is an improved variation of genetic algorithm (GA) that can deal with the problem with a large number of continuous variables and is applied as presented in Algorithm 1. In which, the input of the algorithm is the objective function defined in (39) and algorithm controlling parameters. Specifically, CGA considers a chromosome as a vector of real values, thus is efficient in continuous domains. The k-th chromosome at the t-th generation is

$$\mathbf{d}_k^{(t)} = [\mu_p, \mu_p^{(n)}, h_n], \tag{45}$$

where $n \in \{1, \ldots, N + 1\}$. The algorithm begins with random chromosomes in initial population $\mathbf{d}_k^{(0)}$. Then, each chromosome in the population is evaluated by an objective function and the selection step chooses the good ones for reproduction to maintain the population size λ. In the crossover step, most of chromosomes are recombined in pairs with a crossover rate r_c to create new pairs of chromosomes, called offsprings. Specifically, when CGA chooses a pair of individuals $\mathbf{d}_i^{(t)}$, $\mathbf{d}_j^{(t)}$, it reproduces two new candidates $\mathbf{d}_i^{(t+1)}$, $\mathbf{d}_j^{(t+1)}$ as

$$\mathbf{d}_i^{(t+1)} = (1 - u)\mathbf{d}_i^{(t)} + u\mathbf{d}_j^{(t)}, \tag{46}$$

$$\mathbf{d}_j^{(t+1)} = (1 - u)\mathbf{d}_j^{(t)} + u\mathbf{d}_i^{(t)}, \tag{47}$$

where u is a uniform random value satisfies $0 < u < 1$.

In order to escape from local optima, the mutation step is used to pick several chromosomes at a low mutation rate and modifies them randomly by adding a random value to each entry of the parent chromosomes. This value is governed by a Gaussian distribution whose mean is 0 and scale is r_m. The purpose of this step is to maintain genetic diversity within the population because gene pool

tends to become more and more homogeneous over many generations. Chromosomes evolve through generations as a loop consisting of selection, crossover, and mutation steps in searching space or population. The best chromosome is the output of the optimization process:

$$\mathbf{d}^* = [\mu_p^*, {\mu_p^{(n)}}^*, h_n^*]. \tag{48}$$

5 Numerical Analysis

In this section, numerical results are presented to analyze the OP of the considered NOMA CR and the convergence of Algorithm 1. Without loss of generality, we investigate the considered system with the following system parameters [1,2]. We set the fading parameters to $m_\alpha = 2$, the system bandwidth to $W = 100$ MHz, the number of the URs to $N = 3$, the thresholds of the IDs and PR for successfully decoding their signals are $\gamma_S \in \{3, 5, 7\}$ and $\gamma_P = 10$. Furthermore, we investigate the UR operating in an urban environment with the parameters $\varphi = 9.6177$, $\psi = 0.1581$, $\omega_{\text{LoS}} = 1$, and $\omega_{\text{NLoS}} = 20$ [6].

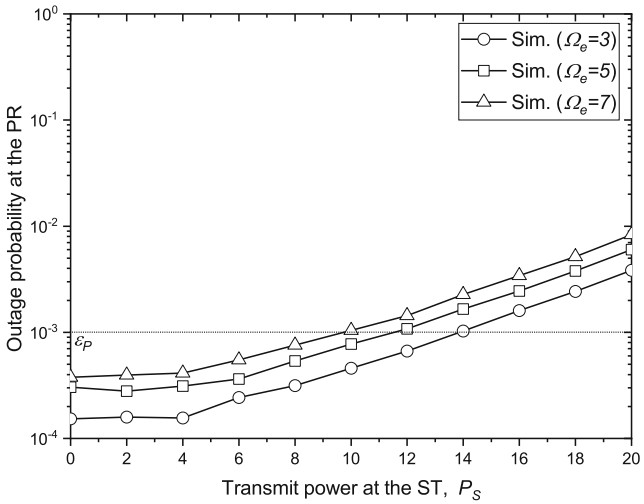

Fig. 2. Impact of the transmit power at the ST and the channel estimation error on the OP of the primary network.

In Fig. 2, we plot the impact of the transmit power at the ST and the channel estimation error on the OP at the PR. It is observed that when we increase P_S and Ω_e, the OP at the PR increases. This is because the high transmit power of the ST and channel estimation error lead the larger interference at the PR. Figure 3 illustrates the throughput of the secondary network for different values of the last UR's altitude and outage threshold γ_S. We can see that $\mathcal{T}_S$ reaches

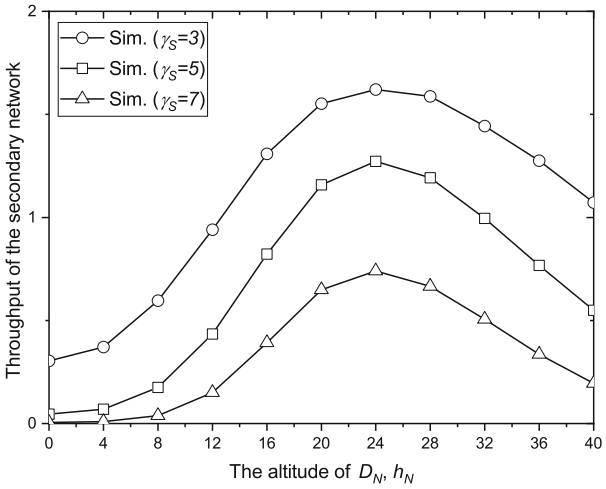

Fig. 3. Impact of the altitude of the last UR and the outage threshold γ_S on the OP of the secondary network.

the optimal point once h_N goes to a specific value. The reason is when the N-th UR flies with high altitude, the probability of the LoS is high. However, if the altitude is very high, the path-loss becomes large.

Table 1. Convergence comparison details

Average generation number to reach 95% maximum value	$r_c = 0.3$	$r_c = 0.5$	$r_c = 0.7$
$r_m = 0.1$	38	22	12
$r_m = 0.2$	66	53	30
$r_m = 0.3$	73	67	57

Next, for CGA optimization part, the results are presented with different combinations of population size $\lambda = \{20, 50, 100\}$, crossover rate $r_c = \{0.3, 0.5, 0.7\}$, and mutation scale $r_m = \{0.1, 0.2, 0.3\}$. Specifically, Fig. 4 portrays the convergence of Algorithm 1 within 60 generations ($T = 60$). Three curves present the mean fitness values over generations for three population sizes of 20, 50, and 100, respectively. It can be seen that the simulation curves all converge after a number of generations, implying that CGA works well with our above mentioned nonlinear optimization problem. Besides, $\lambda = 100$ gives better convergence than $\lambda = 50$ and $\lambda = 20$, or the convergence is more stable with higher population sizes. This is obviously the trade-off between convergence stability and computational cost. It is also remarked from Fig. 4 that all three

curves yield the converged value that matches the maximal value of 1.22 bps/Hz of the second curve ($\gamma_s = 5$) in Fig. 4. This again verifies the reliability of our analysis and CGA implementation.

Table 1 compares the convergence speeds with different combinations of r_c and r_m. λ is fixed to 100 in this experiment set due to the results in Fig. 4. The Table's values are the average generation numbers at which the target function reaches 95% of the optimal system throughput. CGA needs 73 generations for $r_c = 0.3$ and $r_m = 0.3$, while needing only 12 generations for $r_c = 0.7$ and $r_m = 0.1$. Moreover, the convergence is better with larger crossover rate. The reason is with a large enough crossover ratio, the more diverse population will be created; thus, the evolutionary is more convenient. The mutation scale also affects the speed of convergence process. The scale should be small, e.g., at 0.1, so that the fitness function is able to overcome local optima without slowing down the convergence.

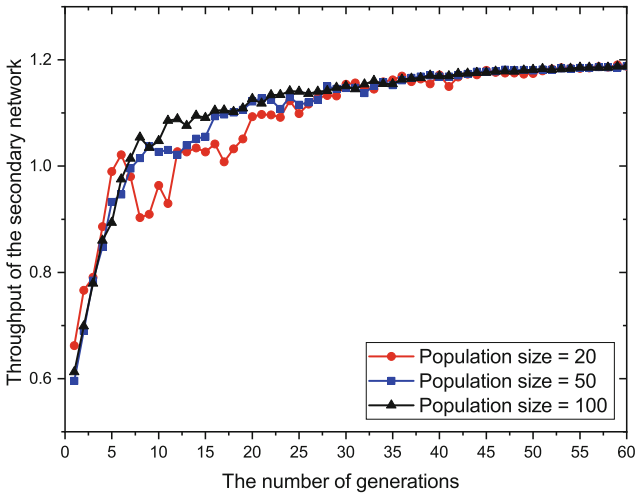

Fig. 4. CGA convergence over generations with different population sizes $\lambda = 20$, 50, and 100.

6 Conclusions

This paper has studied the system performance of a NOMA CR with the help of multiple URs. Accordingly, the expressions for the OP at the PR and the throughput of the secondary network are defined. Based on that, CGA algorithm has been proposed to apply for determining the optimal power allocation and altitudes of the UR to achieve the best throughput under constraints from the primary network. Finally, the numerical results show that the proposed NOMA CR can satisfy the requirements for system performance.

References

1. Bao, V.N.Q., Duong, T.Q., Tellambura, C.: On the performance of cognitive underlay multihop networks with imperfect channel state information. IEEE Trans. Commun. **61**(12), 4864–4873 (2013)
2. Chen, Y., Zhao, N., Alouini, Z.D.M.S.: Multiple UAVs as relays: multi-hop single link versus multiple dual-hop links. IEEE Trans. Wireless Commun. **17**(9), 6348–6359 (2018)
3. Chi-Nguyen, D., Pathirana, P.N., Ding, M., Seneviratne, A.: Secrecy performance of the UAV enabled cognitive relay network. In: Proceedings of International Conference on Communications and Information Technology, pp. 117–121 (2018)
4. Do, D.T., Le, A.T., Lee, B.M.: NOMA in cooperative underlay cognitive radio networks under imperfect SIC. IEEE Access **8**, 86180–86195 (2020)
5. Ji, B., Li, Y., Cao, D., Li, C., Mumtaz, S., Wang, D.: Secrecy performance analysis of UAV assisted relay transmission for cognitive network with energy harvesting. IEEE Trans. Veh. Tech. **69**(7), 7404–7415 (2020)
6. Ji, B., Li, Y., Chen, S., Han, C., Li, C., Wen, H.: Secrecy outage analysis of UAV assisted relay and antenna selection for cognitive network under nakagami-m channel. IEEE Trans. Cogn. Commun. Network. **7**, 1–11 (2020). https://doi.org/10.1109/TCCN.2020.2965945
7. Ji, B., Li, Y., Zhou, B., Li, C., Song, K., Wen, H.: Performance analysis of UAV relay assisted IoT communication network enhanced with energy harvesting. IEEE Access **7**, 38738–38747 (2019)
8. Li, Y., Zhang, R., Zhang, J., Gao, S., Yang, L.: Cooperative jamming for secure UAV communications with partial eavesdropper information. IEEE Access **7**, 94593–94603 (2019)
9. Ozger, M., Pehlivanoglu, E.B., Akan, O.B.: Energy-efficient transmission range and duration for cognitive radio sensor networks. IEEE Trans. Cogn. Commun. Network. 1–1 (2021). https://doi.org/10.1109/TCCN.2021.3130986
10. Prajapat, R., Yadav, R.N., Misra, R.: Energy-efficient k-hop clustering in cognitive radio sensor network for internet of things. IEEE Internet Things J. **8**(17), 13593–13607 (2021)
11. Sboui, L., Ghazzai, H., Rezki, Z., Alouini, M.: On the throughput of cognitive radio MIMO systems assisted with UAV relays. In: Proceedings of the International Wireless Communications and Mobile Computing Conference, pp. 939–944 (2017)
12. Sohail, M.F., Leow, C.Y., Won, S.: Non-orthogonal multiple access for unmanned aerial vehicle assisted communication. IEEE Access **6**, 22716–22727 (2018)
13. Vo, V.N., So-In, C., Tran, D.D., Tran, H.: Optimal system performance in multihop energy harvesting WSNs using cooperative NOMA and friendly jammers. IEEE Access **7**, 125494–125510 (2019)
14. Xiang, Z., Yang, W., Pan, G., Cai, Y., Song, Y.: Physical layer security in cognitive radio inspired NOMA network. IEEE J. Select. Top. Signal Process. **13**(3), 700–714 (2019)